

Photons from anisotropic *Quark-Gluon-Plasma*

Lusaka Bhattacharya^a and Pradip Roy^b
Saha Institute of Nuclear Physics
1/AF Bidhannagar, Kolkata - 700064, INDIA

ABSTRACT

We calculate medium photons due to Compton and annihilation processes in an anisotropic media. The effects of time-dependent momentum-space anisotropy of *Quark-Gluon-Plasma* (QGP) on the medium photon production are discussed. Such an anisotropy can result from the initial rapid longitudinal expansion of the matter, created in relativistic heavy ion collisions. A phenomenological model for the time-dependence of the parton hard momentum scale, $p_{hard}(\tau)$, and anisotropy parameter, $\xi(\tau)$, has been used to describe the plasma space-time evolution. We find significant dependency of photon yield on the isotropization time (τ_{iso}). It is shown that the introduction of early time momentum-space anisotropy can enhance the photon production by a factor of 10 (1.5) (in the central rapidity region) for *free streaming (collisionally-broadened) interpolating* model if we assume fixed initial condition. On the other hand, enforcing the fixed final multiplicity significantly reduces the enhancement of medium photon production.

1 Introduction

One of the goals for the ongoing relativistic heavy ion collision experiments at the Relativistic Heavy Ion Collider (RHIC) and the upcoming experiments at CERN Large Hadron Collider (LHC) is to produce and study the properties of QGP. According to the prediction of lattice quantum chromodynamics, QGP is expected to be formed when the temperature of nuclear matter is raised above its critical value, $T_c \sim 170$ MeV, or equivalently the energy density of nuclear matter is raised above $1 \text{ GeV}/fm^3$ [1]. The possibility of QGP formation at RHIC experiment, with $5 \text{ GeV}/fm^3$ initial density of the created system, is supported by the observation of high p_T hadron suppression (jet-quenching) in the central Au-Au collisions compared to the binary-scaled hadron-hadron collisions [2]. Apart from jet-quenching, several possible probes have been studied in order to characterize the properties of QGP.

However, many properties of QGP are still poorly understood. The most debated question is whether the matter formed in the relativistic heavy ion collisions is in thermal equilibrium or not. The measurement of elliptic flow parameter and its theoretical explanation suggest that the matter quickly comes into thermal equilibrium (with $\tau_{therm} < 1$ fm/c, where τ_{therm} is the time of thermalization) [3]. On the contrary, perturbative estimation suggests

^aE-mail address: lusaka.bhattacharya@saha.ac.in

^bE-mail address: pradipk.roy@saha.ac.in

the slower thermalization of QGP [4]. However, recent hydrodynamical studies [5] have shown that due to the poor knowledge of the initial conditions there is a sizable amount of uncertainty in the estimate of thermalization or isotropization time. It is suggested that (momentum) anisotropy driven plasma instabilities may speed up the process of isotropization [6], in that case one is allowed to use hydrodynamics for the evolution of the matter. However, instability-driven isotropization is not yet proved at RHIC and LHC energies.

In view of the absence of a theoretical proof behind the rapid thermalization and the uncertainties in the hydrodynamical fits of experimental data, it is very hard to assume hydrodynamical behavior of the system from the very beginning. Therefore, one is forced to find out some observables which are sensitive to the early time after the collision. Electromagnetic probes have long been considered as the most effective one to characterize the initial stages of heavy ion collisions. Photons can be one of such observables. Since photons interact only electromagnetically with the plasma, they remain relatively less affected by the later stages of the plasma evolution. Therefore, photons can carry information about the plasma initial conditions [7, 8, 9] only if the observed flow effects from the late stages of the collisions can be understood and modeled properly. The observation of pronounced transverse flow in the photon transverse momentum distribution has been taken into account in model calculations of photon p_T distribution at various beam energies [7, 8, 10, 11, 12]. It is found that because of the transverse kick the low energy photons populate the intermediate regime and consequently, the contribution from hadronic matter becomes comparable with that from the hadronic matter destroying the window where the contribution from QGP was supposed to dominate [12]. Apart from transverse flow effects, the investigation of longitudinal evolution using HBT correlation measurements has been done in Ref. [13]. It is shown that the decrease of R_{side} with p_T (> 2.5 GeV) provides a good indication whether transverse flow is significant or not. However, so far as the pre-equilibrium emission is concerned this effect is not important. Moreover, the elliptical flow (v_2^γ) of photons has recently been calculated in Refs. [14, 15] where it is shown that v_2^γ has a rich structure which reflects the interplay between different emission processes. It is argued that the total photon elliptical flow is small at high p_T implying small elliptical flow during the early stages of the collisions.

For the above mentioned reason photon production from relativistic heavy ion collisions assuming isotropic QGP has been extensively studied [16, 17]. In all these works it is assumed that the plasma thermalizes rapidly with $\tau_{\text{therm}} = \tau_i$ where τ_i is the time scale of parton formation. In spite of equating thermalization time to the parton formation time, in this work we will introduce an intermediate time scale (isotropization time, τ_{iso}) to study the effects of early time momentum-space anisotropy on the medium photon production. The parton formation time τ_i can be estimated from the nuclear saturation scale, i. e. $\tau_i \sim Q_s^{-1}$ [18], where $Q_s \sim 1.5$ (2) GeV for RHIC (LHC). Recently, it has been shown in Ref. [19] that for fixed initial conditions, the introduction of a pre-equilibrium momentum-space anisotropy enhances high energy dileptons by an order of magnitude. To include the time dependent momentum-space anisotropy, we will use the phenomenological model of Ref. [19, 20]. This model assumes two time scales: the parton formation time, τ_i , and the isotropization time, τ_{iso} , which is the time when the system becomes isotropic in momentum space. Immediately after the formation of QGP the system can be assumed to be isotropic [21]. Subsequent rapid expansion of the matter along the beam direction causes faster cooling in the longitudinal direction than in the transverse direction [4]. As a result, the system becomes anisotropic

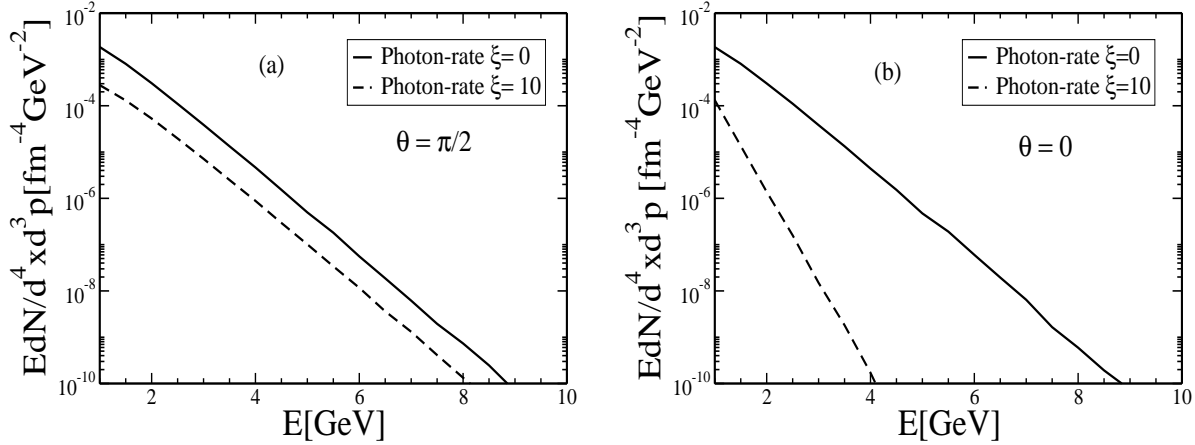


Figure 1: Photon rates for photon propagation angle (a) $\theta = \pi/2$ and (b) $\theta = 0$ as a function of photon energy (E) for two different values of anisotropy parameter ξ with $\alpha_s = 0.3$ and $p_{hard} = 0.446$ GeV

with $\langle p_L^2 \rangle \ll \langle p_T^2 \rangle$ in the local rest frame. At some later time when the effect of parton interaction rate overcomes the plasma expansion rate, the system returns to the isotropic state again and remains isotropic for the rest of the period.

The plan of the paper is the following. We will discuss the medium photon production rate and the space-time evolution of anisotropic QGP in the next section. Section 3 is devoted to describe the results for various evolution scenarios. We summarize in section 4.

2 Formalism

2.1 Photon rate

The lowest order processes for photon emission from QGP are the Compton ($q(\bar{q})g \rightarrow q(\bar{q})\gamma$) and the annihilation ($q\bar{q} \rightarrow g\gamma$) processes. The total cross-section (for both the processes) diverges in the limit $t/u \rightarrow 0$. These singularities have to be shielded by thermal effects in order to obtain infrared safe calculations. It has been argued in Ref. [22] that the intermediate quark acquires a thermal mass in the medium, whereas the hard thermal loop (HTL) approach of Ref. [23] shows that very soft modes are suppressed in a medium providing the natural cut-off $k_c \sim \sqrt{g}T$.

The rate of photon production ($EdN/d^4 x d^3 p$) from anisotropic plasma due to Compton and annihilation processes has been calculated in Ref. [24]. The soft contribution is calculated by evaluating the photon polarization tensor for an oblate momentum-space anisotropy of the system where the cut-off scale is fixed at $k_c \sim \sqrt{g}p_{hard}$. Here p_{hard} is a hard-momentum scale that appears in the distribution functions.

In this work we assume that the infrared singularities can be shielded by the introduction

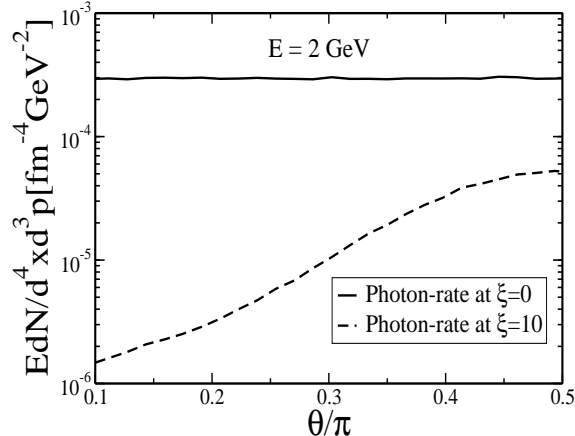


Figure 2: Photon rate as a function of photon propagation angle (θ) for two different value of anisotropy parameter ξ with $\alpha_s = 0.3$ and $p_{hard} = 0.446$ GeV for $E = 2$ GeV.

of the thermal masses for the participating partons. This is a good approximation at times short compared to the time scale when plasma instabilities start to play an important role. We shall see that as long as the static rate is concerned our results are similar to that of Ref. [24]. The differential photon production rate for $1+2 \rightarrow 3+\gamma$ processes in an anisotropic medium is given by [24]

$$E \frac{dN}{d^4 x d^3 p} = \frac{\mathcal{N}}{2(2\pi)^3} \int \frac{d^3 p_1}{2E_1(2\pi)^3} \frac{d^3 p_2}{2E_2(2\pi)^3} \frac{d^3 p_3}{2E_3(2\pi)^3} f_1(\mathbf{p}_1, p_{hard}, \xi) f_2(\mathbf{p}_2, p_{hard}, \xi) \times (2\pi)^4 \delta(p_1 + p_2 - p_3 - p) |\mathcal{M}|^2 [1 \pm f_3(\mathbf{p}_3, p_{hard}, \xi)] \quad (1)$$

where, $|\mathcal{M}|^2$ represent the spin averaged matrix element squared for one of those processes which contributes in the photon rate and \mathcal{N} is the degeneracy factor of the corresponding process. ξ is a parameter controlling the strength of the anisotropy with $\xi > -1$. f_1 , f_2 and f_3 are the anisotropic distribution functions of the medium partons and will be discussed in the following.

In an isotropic system particles move in all directions with equal probability. However, for an anisotropic system there will be atleast one preferred direction. The anisotropic distribution function can be obtained [25] by squeezing or stretching an arbitrary isotropic distribution function along the preferred direction in momentum space,

$$f_i(\mathbf{k}, \xi, p_{hard}) = f_i^{iso}(\sqrt{\mathbf{k}^2 + \xi(\mathbf{k} \cdot \mathbf{n})^2}, p_{hard}) \quad (2)$$

where \mathbf{n} is the direction of anisotropy. It is important to notice that $\xi > 0$ corresponds to a contraction of the distribution function in the direction of anisotropy and $-1 < \xi < 0$ corresponds to a stretching in the direction of anisotropy. In the context of relativistic heavy ion collisions, one can identify the direction of anisotropy with the beam axis along which the

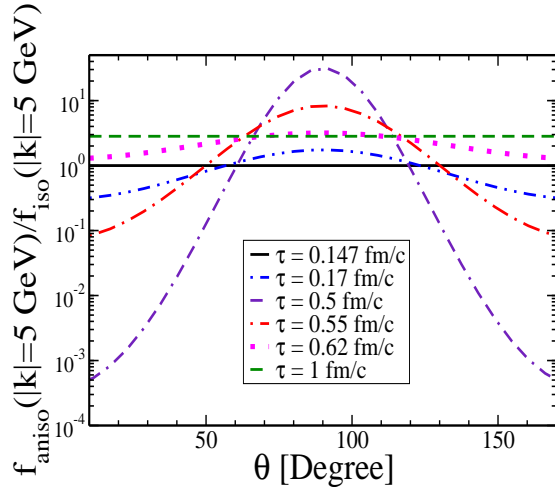


Figure 3: (Color online) $f_{aniso}(|\mathbf{k}| = 5 \text{ GeV})/f_{iso}(|\mathbf{k}| = 5 \text{ GeV})$ as a function of angle (θ) with direction of anisotropy for $\tau_{iso} = 0.5 \text{ fm}$. Different curves correspond to the ratio at different intermediate time.

system expands initially. The hard momentum scale p_{hard} is directly related to the average momentum of the partons. In the case of an isotropic QGP, p_{hard} can be identified with the plasma temperature (T).

2.2 Space time evolution

The previous discussion on the medium photon rate is not enough to make any phenomenological prediction for the expected medium photon yield in an anisotropic QGP as it gives the static photon rate which is also calculated in Ref. [24]. In other words, the rate is not convoluted with the evolution of the matter. To do this one needs to know the time dependence of p_{hard} and ξ . We shall follow the work of Ref. [19] to evaluate the p_T distribution of photons from the first few Fermi of the plasma evolution. Three scenarios of the space-time evolution (as described in Ref. [19]) are the following: (i) $\tau_{iso} = \tau_i$, the system evolves hydrodynamically so that $\xi = 0$ and p_{hard} can be identified with the temperature (T) of the system (till date all the calculations have been performed in this scenario), (ii) $\tau_{iso} \rightarrow \infty$, the system never comes to equilibrium, (iii) $\tau_{iso} > \tau_i$ and τ_{iso} is finite, one should devise a time evolution model for ξ and p_{hard} which smoothly interpolates between pre-equilibrium anisotropy and hydrodynamics. We shall follow scenario (iii) (see Ref. [19] for details) in which case the time dependence of the anisotropy parameter ξ is given by

$$\xi(\tau, \delta) = \left(\frac{\tau}{\tau_i}\right)^\delta - 1 \quad (3)$$

where the exponent $\delta = 2$ ($2/3$) corresponds to *free-streaming (collisionally-broadened)* pre-equilibrium momentum space anisotropy and $\delta = 0$ corresponds to thermal equilibrium. As in Ref. [19], a transition width γ^{-1} is introduced to take into account the smooth transition

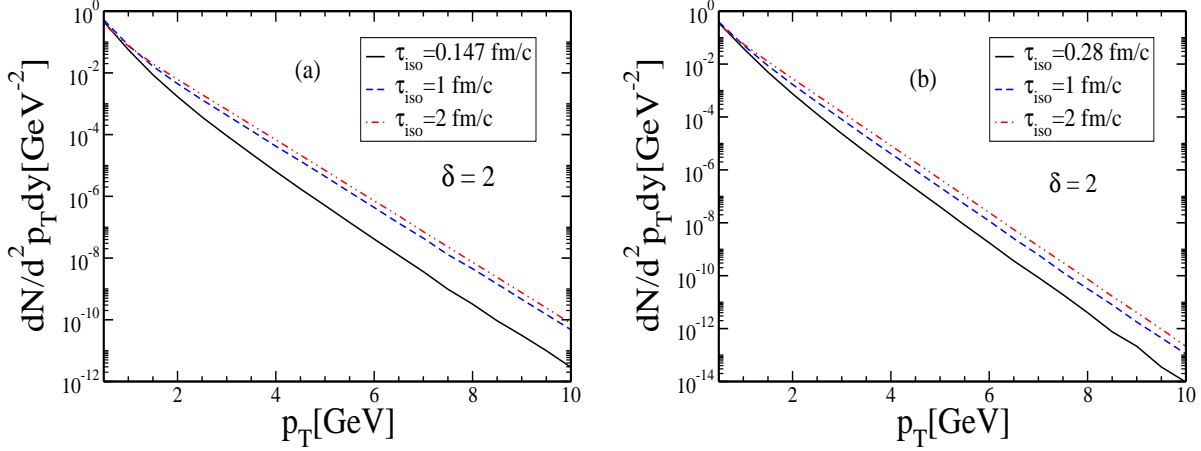


Figure 4: (Color online) Medium photon spectrum, $dN/dy d^2 p_T$, at $\theta = \pi/2$ ($y = 0$) for the *free-streaming interpolating* model ($\delta = 2$) for three different values of isotropization time, τ_{iso} , with initial conditions, (a) Set-I and (b) Set-II .

from non-zero value of δ to $\delta = 0$ at $\tau = \tau_{iso}$. The time dependence of various quantities are, therefore, obtained in terms of a smeared step function [20]:

$$\lambda(\tau) = \frac{1}{2}(\tanh[\gamma(\tau - \tau_{iso})/\tau_i] + 1). \quad (4)$$

For $\tau \ll \tau_{iso}$ ($\gg \tau_{iso}$) we have $\lambda = 0(1)$ which corresponds to *free streaming* (hydrodynamics). With this, the time dependence of relevant quantities are as follows [19]:

$$\begin{aligned} \xi(\tau, \delta) &= \left(\frac{\tau}{\tau_i}\right)^{\delta(1-\lambda(\tau))} - 1, \\ p_{\text{hard}}(\tau) &= T_i \bar{\mathcal{U}}^{1/3}(\tau), \end{aligned} \quad (5)$$

where,

$$\begin{aligned} \mathcal{U}(\tau) &\equiv \left[\mathcal{R} \left(\left(\frac{\tau_{iso}}{\tau} \right)^\delta - 1 \right) \right]^{3\lambda(\tau)/4} \left(\frac{\tau_{iso}}{\tau} \right)^{1-\delta(1-\lambda(\tau))/2}, \\ \bar{\mathcal{U}} &\equiv \frac{\mathcal{U}(\tau)}{\bar{\mathcal{U}}(\tau_i)}, \\ \mathcal{R}(x) &= \frac{1}{2} [1/(x+1) + \tan^{-1} \sqrt{x}/\sqrt{x}] \end{aligned} \quad (6)$$

and T_i is the initial temperature of the plasma. In our calculation, we assume a fast-order phase transition beginning at the time τ_f and ending at $\tau_H = r_d \tau_f$ where $r_d = g_Q/g_H$ is the ratio of the degrees of freedom in the two (QGP phase and hadronic phase) phases and τ_f is obtained by the condition $p_{\text{hard}}(\tau_f) = T_c$ which we take as 170 MeV. We also include the

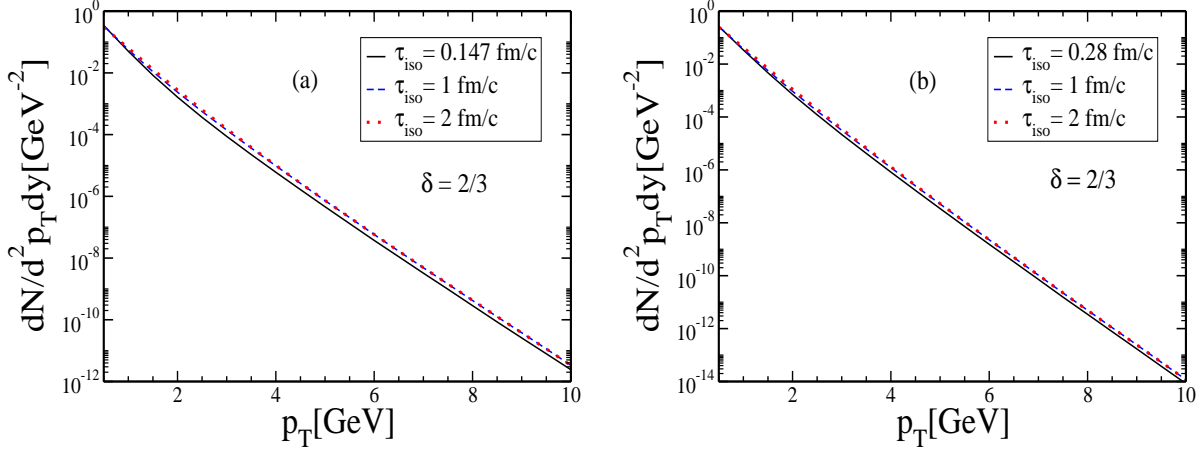


Figure 5: (Color online) Same as Fig. 4 with $\delta = 2/3$.

contribution from the mixed phase. Therefore, the total medium photon yield, arising from pure QGP phase and mixed phase is given by,

$$\frac{dN^\gamma}{dy d^2 p_T} = \pi R_\perp^2 \left[\int_{\tau_i}^{\tau_f} \tau d\tau \int d\eta \frac{dN^\gamma}{d^4 x dy d^2 p_T} + \int_{\tau_f}^{\tau_H} f_{QGP}(\tau) \tau d\tau \int d\eta \frac{dN^\gamma}{d^4 x dy d^2 p_T} \right], \quad (7)$$

where, $f_{QGP}(\tau) = (r_d - 1)^{-1} (r_d \tau_f \tau^{-1} - 1)$, is the fraction of the QGP phase in the mixed phase [26], $R_\perp = 1.2A^{1/3}$ fm is the radius of the colliding nucleus in the transverse plane. The energy of the photon in the fluid rest frame is given by $E_\gamma = p_T \cosh(y - \eta)$ where η and y are the space-time and photon rapidities respectively.

3 Result

To numerically evaluate the medium photon yield in an anisotropic QGP we must have the knowledge of space-time dependence of anisotropy parameter, $\xi(\tau)$, and hard momentum scale, $p_{hard}(\tau)$ as discussed earlier. To include the time dependence of ξ and p_{hard} , we will use Eqs. (5) and (6) described in the previous section (see Ref. [19, 20] for details).

We will now discuss contributions to the total photon yield due to medium photon spectrum from anisotropic QGP with initial conditions that might be achieved at RHIC and LHC energies. In what follows we shall consider two interpolating models: (i) *free-streaming interpolating* model ($\delta = 2$) and (ii) *collisionally-broadened interpolating* model ($\delta = 2/3$). To cover the uncertainties in the initial conditions for a given beam energy, we consider two sets of initial conditions, one at a relatively high temperature of $T_i = 0.446$ GeV and a relatively short initial time of $\tau_i = 0.147$ fm/c denoted hereafter by Set-I, and another at a lower temperature $T_i = 0.350$ GeV and somewhat later initial time of $\tau_i = 0.28$ fm/c denoted hereafter by Set-II. The *free-streaming interpolating* model with fixed initial conditions (FIC) leads to entropy generation [19] and, therefore, the allowed values of τ_{iso} , in this

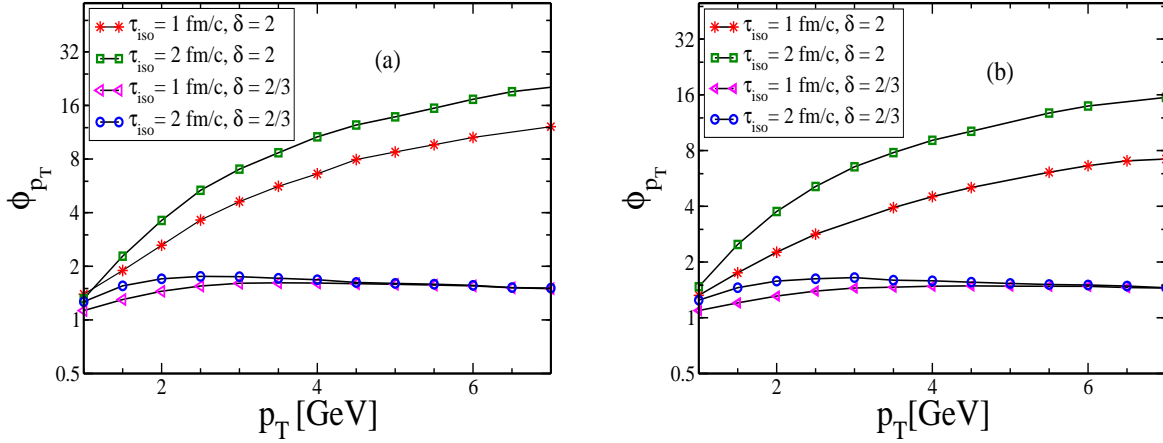


Figure 6: (Color online) *Photon enhancement factor* (ϕ_{p_T}) as a function of photon transverse momentum (p_T) for the *free-streaming* and *collisionally-broadened interpolating* models with fixed initial conditions. (a) and (b) correspond to Set-I and Set-II respectively.

case, is much more constrained. On the other hand, for *collisionally-broadened interpolation* model, the upper bound on τ_{iso} is much larger due to small amount of entropy generation. The estimates of upper bounds on τ_{iso} for both the models are listed in Ref. [19].

We also invoke the conditions of fixed final multiplicity (fixed entropy) to calculate the photon yield from the plasma. In such case, the initial hard momentum scale ($p_{\text{hard}}(\tau_i)$) will be τ_{iso} dependent, i.e. the larger the value of τ_{iso} smaller will be the initial hard momentum scale. Therefore, the enhancement in the yield will be less as compared to the case of fixed initial conditions. Moreover, as we shall see, for a given condition the enhancement will be lower in case of *collisionally-broadened* model as δ is smaller (close to isotropic expansion).

Fig. 1 shows the medium photon production rate (static) as a function of photon energy, E , for two different values of the anisotropy parameter, ξ , and two different values of photon angle, θ . We have used $\alpha_s = 0.3$ and $p_{\text{hard}} = 0.446$ GeV. It is clear from Fig. 1 that the photon rate is more suppressed in the direction parallel to the direction of anisotropy compared to the transverse direction for an anisotropic QGP. This is due to the fact that for $\xi > 0$, decreasing value of photon angle (θ) implies decreasing value of medium parton density and hence decreasing photon rate as can be seen from Eq. (2). This is also clear from Fig. 2, which shows the photon rate as a function of photon angle, (θ), for $E = 2$ GeV for two different values of ξ . It is observed that for a given anisotropy parameter, the value of the photon rate is larger in the transverse direction. However, the photon rate in an oblate anisotropic medium ($\xi > 0$) is always small compared to the photon rate in an isotropic medium. This can be attributed to the fact that an oblate anisotropic distribution (Eq. 2) i.e. *+ve* value of ξ corresponds to the suppression of medium parton density. As a result, introduction of anisotropy (with *+ve* value of anisotropy parameter (ξ)), in general, leads to a suppression of medium photon rate (static).

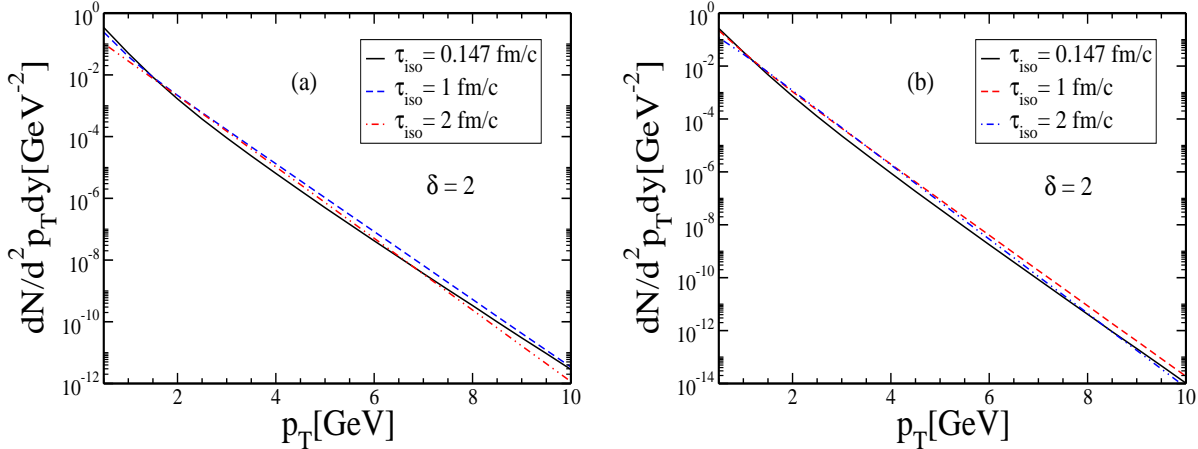


Figure 7: (Color online) Same as Fig. 4 with FMM

After the very short discussion of the medium photon rate in an anisotropic QGP, we will now discuss the effects of pre-equilibrium momentum space anisotropy of the QGP on the thermal photon spectrum. To illustrate the effects of pre-equilibrium momentum space anisotropy of QGP on the parton densities, in Fig. 3, we have plotted the ratio (f_{aniso}/f_{iso}) (for $|\mathbf{k}| = 5$ GeV) as a function of the angle between \mathbf{k} (the momentum of the plasma parton) and \hat{n} (the direction of anisotropy) for different values of intermediate time with $\tau_{iso} = 0.5$ fm. Here $f_{aniso}(\mathbf{k}, p_{hard})$ is the parton distribution function for a QGP with pre-equilibrium momentum space anisotropy and $f_{iso}(\mathbf{k}, p_{hard})$ is the parton distribution function for a QGP without any pre-equilibrium momentum space anisotropy. The anisotropic distribution functions, in Fig. 3, are calculated in the framework of fixed initial condition *free-streaming interpolation* model with $\delta = 2$. Fig. 3 clearly shows an enhancement of anisotropic distribution in the transverse direction and suppression in the longitudinal direction for $\tau < \tau_{iso}$. The enhancement in the transverse direction is a consequence of the enhancement of the hard momentum scale, p_{hard} , for $\tau < \tau_{iso}$. However, in the longitudinal direction, the suppression due to the nonzero value of the anisotropy parameter does not stand over the enhancement due to the enhanced value of hard momentum scale.

3.1 Photon spectrum for fixed initial conditions with $\delta = 2$ and $\delta = 2/3$

In this section we will present the medium photon spectrum assuming fixed initial condition and *free streaming (collisionally-broadened) interpolating* model with $\delta = 2$ (2/3). In Fig. 4 we have presented the medium photon yield in the mid rapidity ($\theta_\gamma = \pi/2$) as a function of photon transverse momentum at for those two sets of fixed initial conditions. Fig.4a (4b) corresponds to $T_i = 0.446$ (0.350) GeV and $\tau_i = 0.147$ (0.28) fm/c. In estimating these results, we have used $\alpha_s = 0.3$. Different lines in Fig. 4 correspond to different isotropization

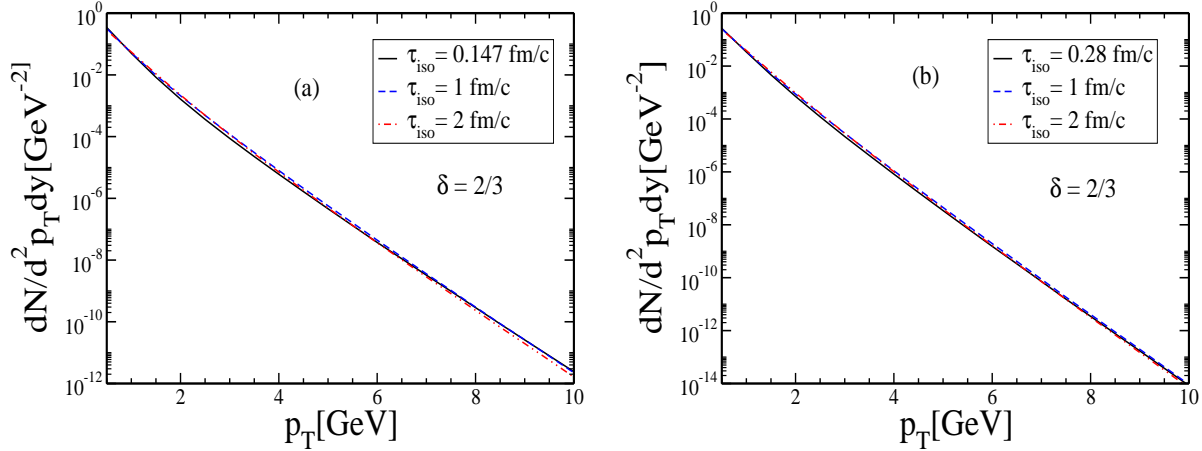


Figure 8: (Color online) Same as Fig. 5 with FMM

times, τ_{iso} . We observe enhancement of photon yield when $\tau_{iso} > \tau_i$. The enhancement of photon yield in the transverse directions is due to the fact that momentum-space anisotropy enhances the density of plasma partons moving at the mid rapidity as can be seen from Fig. 3.

In Fig. 5, we have shown the predicted photon yields (at the mid rapidity) for a given beam energy (with two different sets of initial conditions) assuming the time dependence of the hard momentum scale and anisotropy parameter as given by Eq. 5 with $\delta = 2/3$. It is important to mention that $\delta = 2/3$ corresponds to *collisionally-broadened interpolating* model. Fig. 5 shows enhancement of photon yield as we increase the isotropization time. However, compared to the FIC *free-streaming interpolating* model, discussed in the previous para, here, the enhancement of the photon yield is small. This is due to the fact that in the case of *collisionally-broadened interpolating* model we have included the possibility of momentum space broadening of the plasma partons due to interactions. *Collisionally broadened interpolating* model is close to thermal equilibrium. As a result the yield is close to the equilibrium value.

To quantify the effect of isotropization time, we define *photon enhancement* factor $\Phi(p_T)$ as [19]:

$$\Phi(\tau_{iso}, \theta) = \left(\frac{dN(\tau_{iso})}{dy d^2 p_T} \right)_\theta / \left(\frac{dN(\tau_{iso} = \tau_i)}{dy d^2 p_T} \right)_\theta, \quad (8)$$

which is plotted in Fig. 6 as a function of the photon transverse momentum. Fig. 6a (6b) for $T_i = 0.446$ GeV and $\tau_i = 0.147$ fm/c ($T_i = 0.350$ GeV and $\tau_i = 0.28$ fm/c) shows that for the fixed initial condition *free-streaming interpolating* model, the photon yield at $p_T = 5$ GeV is enhanced by a factor of 13.8 (11.5) at mid rapidity at $\tau_{iso} = 2$ fm/c. Fig. 6 also includes the photon enhancement factor for FIC collisionally broadened interpolating model. However, in the frame work of FIC *collisionally-broadened interpolation* model, enhancement of photon yield is marginal at $\tau_{iso} = 2$ fm/c.

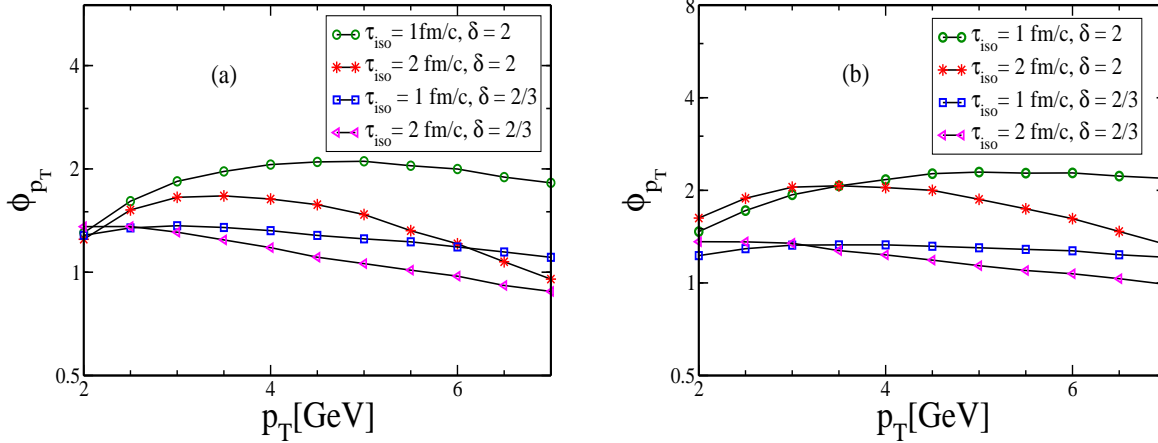


Figure 9: (Color online) Same as Fig. 6 with FMM

3.2 Photon spectrum for fixed final multiplicity (FMM) with $\delta = 2$ and $\delta = 2/3$

In the previous section we have used the two interpolating models which assumes fixed initial conditions. However, enforcing fixed initial condition results in generation of particle number and enhance the final multiplicity. Starting with a fixed initial condition, the interpolating model (discussed in section 2.2) corresponds to a hard momentum scale (for $\tau \gg \tau_{iso}$) which is larger by a factor of $[\mathcal{R}((\tau_{iso}/\tau_i)^\delta - 1)]^{0.25}$ compared to the momentum scale results from the free hydrodynamic expansion of a system (with the same initial condition) from the beginning. To ensure fixed final multiplicity in this model one has to redefine $\bar{\mathcal{U}}(\tau)$ in Eq. 5 as in [19]:

$$\bar{\mathcal{U}}(\tau) = \frac{\mathcal{U}(\tau)}{\mathcal{U}(\tau_i)} \left[\mathcal{R}((\tau_{iso}/\tau_i)^\delta - 1) \right]^{-3/4} (\tau_i/\tau_{iso})$$

This redefinition corresponds to a lower initial hard momentum scale ($p_{hard}(\tau_i) < T_i$) for $\tau_{iso} > \tau_i$. Larger value of isotropization time corresponds to lower initial hard momentum scale.

The transverse photon yields assuming FMM and *free-streaming interpolating* model are presented in Fig. 7 as a function of photon transverse momentum for different values of isotropization times with the initial conditions Set I (Fig.7a) and Set II (Fig.7b). In the case of fixed initial condition (*free-streaming* or *collisionally-broadened*) interpolating model we have obtained significant enhancement of transverse photon yield due to the pre-equilibrium momentum space anisotropy of QGP. However, fixing the final multiplicity significantly reduce the effect of pre-equilibrium anisotropic phase. Moreover as a result of fixing final multiplicity we obtain a suppression of photon yield in the high p_T region. One more interesting consequence of fixing final multiplicity is that larger isotropization time corresponds to suppression in the high p_T region and less enhancement in the intermediate p_T region.

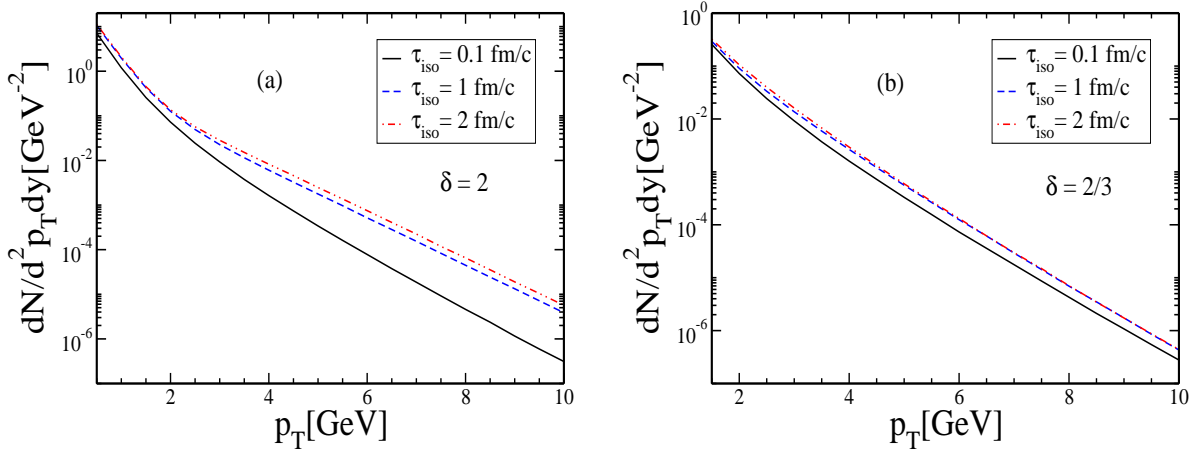


Figure 10: (Color online) Medium photon spectrum, $dN/d^2 p_T dy$, at $\theta = \pi/2 (y = 0)$. (a) ((b)) corresponds to *free streaming interpolating model* (*collisionally-broadened interpolating model*) for three different values of isotropization time, τ_{iso} , with initial temperature $T_i = 0.828$ GeV and initial time $\tau_i = 0.1$ fm/c.

This is due to the fact that to ensure the fixed final multiplicity in the pre-equilibrium *free streaming interpolating* model, one has to reduce the initial hard momentum scale or equivalently the initial energy density.

The photon yield for two sets of initial conditions, assuming *collisionally-broadened* ($\delta = 2/3$) pre-equilibrium phase of QGP with fixed final multiplicity is displayed in Fig. 8. It is observed that fixing final multiplicity significantly reduce the effects of *collisionally-broadened* pre-equilibrium phase of QGP. As discussed in the previous section, this is again due to the fact that in order to maintain fixed final multiplicity for $\tau_{iso} > \tau_i$ the initial energy density (or equivalently initial hard momentum scale) has to be reduced.

In order to see the difference between FIC and FMM we plot Φ_{p_T} with FMM condition, in Fig. 9 both for $\delta = 2$ and $\delta = 2/3$. Since the *collisionally-broadened interpolating* model is always closer to local-isotropic expansion, this results in less photon enhancement compared to the *free-streaming* pre-equilibrium phase (also see Fig. 6). For the initial condition Set-I (Set-II) we predict an enhancement of the order of 1.6 (1.53) for $p_T = 5$ GeV as a result of *collisionally-broadened* pre-equilibrium phase with fixed final multiplicity as we vary τ_{iso} from τ_i to 2 fm/c, whereas *free-streaming* pre-equilibrium phase with fixed final multiplicity corresponds to a enhancement (for $p_T = 5$ GeV) by a factor of 2.1 (1.13).

3.3 Photon yield for fixed initial conditions with higher initial temperature

To demonstrate the effect of higher initial temperature (might be relevant for LHC energies) we proceed to calculate the photon yield with FIC for both the *free streaming* ($\delta = 2$) and

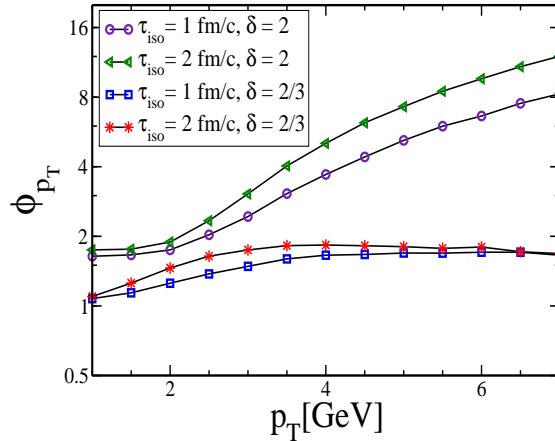


Figure 11: (Color online) *Photon enhancement factor* (ϕ_{p_T}) as a function of photon transverse momentum (p_T) for the *free streaming* and *collisionally-broadened interpolating* models ($\delta = 2, 2/3$) with fixed initial condition for two different values of isotropization time (τ_{iso}) with $T_i = 0.828$ GeV and $\tau_i = 1$ fm/c.

collisionally broadened ($\delta = 2/3$) *interpolating* models. The transverse momentum distribution of medium photons in central rapidity region with $T_i = 0.828$ GeV and $\tau_i = 0.1$ fm/c is displayed in Fig. 10. Here also *free-streaming* pre-equilibrium phase corresponds to more enhancement compared to the *collisionally-broadened* pre-equilibrium phase. In Fig. 11, we have plotted the photon *enhancement factors* (for two different values of isotropization time) as a function of photon transverse momentum both for the *free-streaming* and *collisionally-broadened* interpolating model with fixed initial condition. Fig. 11 shows an enhancement (for $p_T = 5$ GeV) of transverse photon yield by a factor of 7.3 (1.8) at $\tau_{iso} = 2$ fm/c for fixed initial condition *free-streaming* (*collisionally-broadened*) *interpolating* model.

It should be noted that in order to apply our calculations to explain the experimental data we should add to this the contributions from various other sources of photon productions. The model used for this purpose should properly include the effects of transverse flow as it affects the photon spectra significantly. Applications of the present work to calculate the photon p_T distribution at RHIC and LHC energies incorporating transverse flow effects is in progress and will be reported elsewhere [27].

4 Conclusion

To summarize, we have investigated the effects of the pre-equilibrium momentum space anisotropy of the QGP on the medium photon production due to Compton and annihilation processes with various initial conditions. To describe the transition of the plasma from initial non-equilibrium state to an isotropic thermalized state, we have used two phenomenological models for the time dependence of the hard momentum scale (p_{hard}) and plasma anisotropy

parameter (ξ). The first model is based on the assumption of fixed initial condition. However, enforcing fixed initial condition causes entropy generation. Therefore, we have also considered a second model which assumes fixed final multiplicity. Both the possibilities of *free streaming* and *collisionally broadened* pre-equilibrium phase of the QGP are considered. To cover the uncertainties in the initial conditions for for a given beam energy, we have used two sets of initial conditions, one at a relatively high temperature and a relatively short initial time and other at a lower temperature and somewhat later initial time.

We estimate the p_T distribution of photons for different isotropization times in the frame work of these phenomenological models. It is found that, for fixed initial condition, a *free-streaming* interpolating model can enhance the thermal photon yield by an order of magnitude at higher p_T . However, for *collisionally broadened* pre-equilibrium phase with fixed initial condition, the enhancement of photon yield is not that much. This is due to the fact that the energy density, hard momentum scale and anisotropy parameter corresponding to the *collisionally broadened* interpolating model are always closer to the local isotropic expansion. Since fixing the final multiplicity reduce the initial hard momentum scale or equivalently the initial energy density, the enhancement of the photon yield is significantly reduced (both for the *free streaming* and *collisionally broadened* interpolating models). Moreover, for fixed final multiplicity, we predict a suppression of thermal photon yield in the low and high transverse momentum region as has been observed in the case of dilepton invariant mass spectrum for anisotropic plasma [19].

References

- [1] F. Karsch, Nucl. Phys. **A698**, 199 (2002).
- [2] J. D. Bjorken, Fermilab-Pub-82/59-THY(1982) and Erratum (Unpublished); M. Gyulassy, P. Levai and I. Vitev, Nucl. Phys. B **571**, 197 (2000); B. G. Zakharov, JETP Lett. **73**, 49 (2001); M. Djordjevic and U. Heinz, Phys. Rev. Lett **101**, 022302 (2008); G -Y Qin, J. Ruppert, C. Gale, S. Jeon, G. Moore, and M. G. Mustafa, Phys. Rev. Lett **100**; R. Baier *et al.*, J. High Ener. Phys. **0109**, 033 (2001); S. Jeon and G. D. Moore, Phys. Rev. **C71**, 034901 (2005); A. K. Dutt-Mazumder, J. Alam, P. Roy, and B. Sinha, Phys. Rev. D **71**, 094016 (2005); P. Roy, J. Alam, and A. K. Dutt-Mazumder, J. Phys. G. **35**, 104047 (2008).
- [3] U. W. Heinz, arXiv:nucl-th/0512051.
- [4] R. Baier, A. H. Muller, D. Schiff and D. T. Son, Phys. Lett. **B502**, 51 (2001).
- [5] M. Luzum and P. Romatschke, arXiv:0804.4015 [nucl-th].
- [6] S. Mrowczynski, Phys. Lett. **B314** 118 (1993); S. Mrowczynski, Acta. Phys. Pol. B **37**, 427 (2006); P. Arnold, J. Lenghan, G. D. Moore and L. G. Yaffe, Phys. Rev. Lett. **94**, 072302 (2005); A. Rebhan, P. Romatschke and M. Strickland, Phys. Rev. Lett. **94**, 102303 (2005); P. Romatschke and R. venugopalan, Phys. Rev. Lett **96**, 062302. (2006)

- [7] J. Alam, J. K. Nayak, P. Roy, A. K. Dutt-Mazumder, and B. Sinha, *J. Phys. G* **34**, 871 (2007).
- [8] D. K. Srivastava, *Eur. Phys. J. C* **10**, 487 (1999).
- [9] P. Hovinen, P. V. Ruuskanen, and S. S. Rasanen, *Phys. Lett. B* **535**, 109 (2002).
- [10] J. Cleymens, K. Redlic, and D. K. Srivastava, *Phys. Rev. C* **55**, 1431 (1997).
- [11] J. Alam, S. Sarkar, T. Hatsuda, T. K. Nayak, and B. Sinha, *Phys. Rev. C* **63**, 021901(R) (2001).
- [12] T. Renk, hep-ph/0408218.
- [13] T. Renk, *Phys. Rev. C* **71**, 064905 (2005).
- [14] U. Heinz, R. Chatterjee, F. Frodermann, C. Gale, and D. K. Srivastava, *Nucl. Phys. A* **783**, 379c (2007).
- [15] S. Turbide, C. Gale, and R. J. Fries, *Phys. Rev. Lett.* **96**, 032303 (2006)
- [16] J. Kapusta, P. Iichard and D. Seibert, *Phys. Rev. D* **44**, 2774 (1991).
- [17] J. Alam, S. Sarkar, P. Roy, T. Hatsuda and B. Sinha: *Annals of Phys.* **286**, 159 (2000).
- [18] R. Venugopalan, arXiv:0707.1867v2 [hep-ph].
- [19] M. Martinez and M. Strickland, arXiv:0805.4552 [hep-ph].
- [20] M. Martinez and M. Strickland, *Phys. Rev. Lett.* **100**, 10231 (2008).
- [21] W. Jas and S. Mrowczynski, *Phys. Rev. C* **76**, 044905 (2007).
- [22] K. Kajantie and P. V. Ruuskanen, *Phys. Lett. B* **121**,352 (1983).
- [23] R. D. Pisarki and E. Braaten, *Nucl. Phys B* **337**, 569 (1990); *ibid Nucl. Phys. B* **339**,310 (1990).
- [24] B. Schenke and M. Strickland *Phys. Rev. D* **76**, 025023 (2007).
- [25] P. Romatschke and M. Strickland, *Phys. Rev. D* **69**, 065005 (2004).
- [26] K.Kajantie, J. Kapusta, L. McLerran and A. Mekjian, *Phys. Rev D* **34**, 2746 (1986).
- [27] L. Bhattacharya and P. Roy, in preparation.